DOE/PC/92536--T14

Oxidation of Substituted Phenols in Supercritical Water

Final Technical Report

Reporting Period Start Date: September 1992

Reporting Period End Date: August 1996

Principal Author: Phillip E. Savage

Date Issued: November 1996

DOE Award Number: DE-FG22-92PC92536

Submitted by: Phillip E. Savage
Associate Professor
Chemical Engineering Department
University of Michigan
Ann Arbor, MI 48109-2136

Disclaimer

ABSTRACT

Wastewaters from coal-conversion processes contain phenolic compounds in appreciable concentrations. These compounds need to be removed so that the water can be discharged or re-used. Oxidation in supercritical water is one potential means of treating coal-conversion wastewaters, and this project examined the reactions of model pollutants in supercritical water. The decomposition of cresols, hydroxybenzaldehydes, nitrophenols, and benzenediols was studied in dilute aqueous solutions in both the presence and absence of oxygen at 460°C and 250 atm.

Thermolysis (no O_2) under these conditions produced conversions of less than 10% for *o*-, *m*-, and *p*-cresol, whereas hydroxybenzaldehydes and nitrophenols were much more reactive. Global rate expressions are reported for the thermolysis of each hydroxybenzaldehyde and nitrophenol isomer. Phenol was a major product from the thermal decomposition of all of the substituted phenols studied. For a given substituent, *o*-substituted phenols reacted more rapidly than the other isomers. For a given substituted position, nitrophenols reacted more rapidly than hydroxybenzaldehydes, which in turn reacted more rapidly than cresols. These results demonstrate that the treatment of CHO- and NO_2-substituted phenols by oxidation in supercritical water will involve the oxidation of thermal decomposition products in addition to the oxidation of the original compounds.

Experimental data from the oxidation of these compounds were fit to global, power-law rate expressions. The resulting rate laws showed that the reactivity of the different isomers at 460°C was in the order of *ortho* > *para* > *meta* for cresols and hydroxybenzaldehydes. Moreover, the CHO-substituted phenol was more reactive than the analogous CH_3-substituted phenol, and all of these substituted phenols were more reactive than phenol itself. Identifying and quantifying the reaction products of incomplete oxidation allowed us to assemble a general reaction network for the oxidation of cresols in supercritical water. This network comprises parallel primary paths to phenol, to a hydroxybenzaldehyde, and to ring-opening products. The hydroxybenzaldehyde reacts through parallel paths to phenol and to ring-opening products. Phenol also reacts via two parallel paths, but these lead to phenol dimers and ring-opening products. The dimers are eventually converted to ring-opening products, and the ring-opening products are ultimately converted to CO_2. The relative rates of the different paths in the reaction network are strong functions of the location of the substituent on the phenolic ring.

TABLE OF CONTENTS

1. EXECUTIVE SUMMARY

Substituted phenols, which are compounds representative of those commonly found in coal conversion wastewaters, were oxidized in supercritical water (SCW). Both oxidative and non-oxidative decomposition routes were examined. The objective of this experimental research was to obtain the reaction engineering information required to enable supercritical water oxidation of coal-conversion wastewaters to be evaluated as a potential treatment technology.

Cresols are largely stable in SCW at 460°C and 250 atm. In contrast, hydroxybenzaldehydes and nitrophenols are reactive under these conditions. Thus, treatment of these compounds by SCW oxidation will involve a significant thermal component, which implies that much of the oxidation will be of the thermal reaction products (such as phenol) rather than the substituted phenol itself.

For phenols with CHO and NO_2 substituents, the *o*-substituted isomer is the most reactive in SCW. For a given substituent location, nitrophenols are more reactive than hydroxy-benzaldehydes, which are much more reactive than cresols. Thus, there are clearly substituent effects on the reactivity of substituted phenols in SCW. This observation suggests that quantitative structure-reactivity relations might be available for this class of compounds.

The oxidation of CH_3- and CHO-substituted phenols in supercritical water proceeds more rapidly than the oxidation of phenol itself. For a given substituent, *o*-substituted phenols are the most reactive, and *m*-substituted phenols are least reactive. For a given point of substitution, CHO-substituted phenols are more reactive than CH_3-substituted phenols. Quantitative reaction rate laws for the oxidation of each phenolic compound appear in this report.

The oxidation of cresols in supercritical water proceeds through three parallel paths, demethylation (to form phenol), oxidation of the methyl group (to form hydroxybenzaldehyde), and ring-opening. The ring-opening path most likely proceeds through carboxylic acid intermediates, the decarboxylation of which account for the high yields of CO_2. The relative rates of the three parallel paths are isomer specific and consistent with the bond energies and resonance stabilization expected in substituted phenols. The oxidation of hydroxybenzaldehydes in supercritical water proceeds through two parallel paths. One path leads to phenol and the other involves ring-opening and CO_2 formation.

2. INTRODUCTION

Supercritical water oxidation (SCWO) is a waste-treatment process that converts organic carbon to CO_2 at reaction conditions that exceed the critical point of water (T_C = 374 °C, P_C = 218 atm.). Water above its critical point is a good solvent for both oxygen and organic compounds, which allows these components to react quickly in a homogeneous fluid phase (Modell, 1989).

Information about the kinetics and byproducts from oxidation of real aqueous pollutants is essential for the design of reliable commercial SCWO reactors. A knowledge of the reaction kinetics allows one to calculate the residence times required for a desired destruction and removal efficiency in a commercial SCWO reactor. A knowledge of the identities and yields of reaction products allows one to identify processing conditions that minimize the production of undesired intermediate byproducts.

Savage et al. (1995) review previous SCWO research with model pollutants, and that review showed that phenolic compounds are the model pollutants studied most extensively at SCWO conditions. This attention is a reflection of phenol and substituted phenols having high water solubilities, which cause them to appear in industrial wastewaters including those from coal-conversion processes (e.g., Yen et al., 1982; Jevtitch and Bhattacharyya, 1986). Even though phenolic compounds have received some attention, most of this attention has focused on treatability studies rather than more fundamental reaction engineering investigations. The limited information available on the reaction kinetics and pathways for substituted phenols in supercritical water and the importance of these compounds in coal-conversion wastewaters motivated this study of the reactions of substituted phenols in supercritical water.

The types of reactions that can occur under SCWO conditions include pyrolysis, hydrolysis, and oxidation. The first two reactions can proceed even in the absence of an added oxidant. If the rates of these reactions are sufficiently rapid, then the compounds that are ultimately oxidized could be the hydrolysis and pyrolysis products of the target compound rather than the compound itself. Clearly, an understanding of both the oxidative and non-oxidative decomposition reactions of organic compounds in SCW would facilitate the safe treatment of wastes by SCWO.

3. EXPERIMENTAL SECTION

The organic reactants were obtained either from Aldrich Chemical Co. or Eastman Chemical Co. in high purity and used as received. Aqueous stock solutions on the order of 100 - 1000 ppm were made for each of these compounds. These solutions served as the reactor feed.

The experiments were performed in a nominally isothermal, isobaric, plug-flow reactor constructed with Hastelloy C276 tubing. The reactor system contained separate 1.08 mm. I.D. preheat sections for aqueous feed streams containing the organic compound and oxygen. The preheated feed streams mixed at the entrance to the reactor, which was either a one- or a four-meter length of 1.40 mm. I.D. tubing. Two different lengths were used to facilitate exploring a sufficiently wide range of residence times. The preheat lines and reactor tubing were immersed in a temperature-controlled fluidized sand bath operating at the desired reaction temperature.

The reactor effluent was rapidly cooled and returned to ambient conditions prior to analysis. The gaseous products were analyzed with an on-line gas chromatograph equipped with a thermal conductivity detector. We used high performance liquid chromatography (HPLC) with UV detection to measure the concentrations of the phenolic compounds in both the reactor feed and in the aqueous reactor effluent. Other aqueous-phase reaction intermediates were identified from analyses employing a gas chromatograph (GC) with a mass spectrometric detector and then quantified from analyses employing a GC with a flame ionization detector. The reactor system and analytical protocol are described in much greater detail elsewhere (Martino et al., 1995; Thornton and Savage, 1990).

Molar yields of products were calculated as the molar flow rate of the product in the reactor effluent divided by the molar flow rate of reactant into the reactor. We estimate the run-to-run variability in the molar yields to be about $\pm$ 15%. We also calculated a carbon tally as the percentage of carbon atoms in the feed that appear in quantified products in the reactor effluent. A carbon tally of 100% corresponds to all of the carbon fed to the reactor appearing in the quantified products in the effluent.

The residence times for these experiments were calculated as the reactor volume divided by the volumetric flow rate at reaction conditions. This approach provides a consistent basis for the residence time, but it is a lower bound for the thermolysis experiments because it neglects the amount of time the fluid spends in the preheat line as it reaches the reaction temperature.

4. RESULTS AND DISCUSSION

4.1 THERMOLYSIS IN SUPERCRITICAL WATER

We conducted both thermolysis and oxidation reactions of several phenolic compounds in SCW at the nominal reaction conditions of 460°C and 250 atm. We used cresols, hydroxybenzaldeydes, nitrophenols, and dihydroxybenzenes as reactants, substituted phenols that have but a single substituent located at either the *ortho-*, *meta-* or *para-* position relative to the OH group. We will first present results from the thermolysis experiments (no oxygen present) and then present results from oxidation experiments.

4.1.1 Thermolysis of Cresols

Tables 1–3 summarize the experimental results for *o-*, *m-*, and *p*-cresol. The cresol thermolysis products that were identified and quantified are phenol and the corresponding hydroxybenzaldehyde (HB). Consistent with our earlier report (Martino et al., 1995), the thermal decomposition of *o*-cresol led to conversions of <10% for the conditions studied. In fact, five of the six experiments led to conversions less than 4%, whereas only one experiment gave a conversion near 10%. *p*-Cresol exhibited conversions that reached nearly 9%, whereas the *m*-cresol conversion was always significantly lower. Because the cresols were largely thermally stable under SCW processing conditions, we did not acquire additional data or attempt to develop reaction rate laws.

Table 1: Summary of *o*-cresol thermolysis in SCW at 460°C and 250 atm.

	Concentration		Product Yields		
Residence Time (s)	*o*-cresol (μmol/L)	Conversion (%)	*o*-HB (%)	Phenol (%)	Carbon Tally (%)
1.3	257.	1.8	n.d.	1.6	99.6
3.0	257.	3.5	n.d.	3.1	99.2
6.6	258.	3.8	n.d.	5.5	100.9
8.0	267.	1.4	n.d.	2.1	100.4
15	268.	9.8	n.d.	1.3	91.3
38	267.	3.1	n.d.	2.5	99.1

Table 2: Summary of *m*-cresol thermolysis in SCW at 460°C and 250 atm.

	Concentration		Product Yields		
Residence Time (s)	*m*-cresol (μmol/L)	Conversion (%)	*m*-HB (%)	Phenol (%)	Carbon Tally (%)
1.4	94.6	0.6	0.0	0.0	99.4
3.1	94.5	2.3	0.0	0.0	97.7
6.7	94.7	2.9	0.3	0.0	97.3

Table 3: Summary of *p*-cresol thermolysis in SCW at 460°C and 250 atm.

	Concentration		Product Yields		
Residence Time (s)	*p*-cresol (μmol/L)	Conversion (%)	*p*-HB (%)	Phenol (%)	Carbon Tally (%)
1.3	186.	3.0	0.1	0.3	97.3
3.1	185.	8.8	1.0	1.1	93.1
6.7	186.	7.1	0.7	1.1	94.5

4.1.2 Thermolysis of Hydroxybenzaldehydes

Tables 4 – 6 summarize the results from the experiments with *o*-, *m*-, and *p*-hydroxybenzaldehyde. Pyrolysis or hydrolysis reactions are much more significant for the disappearance of hydroxybenzaldehydes than for cresols. Phenol was formed in high yields and nearly 100% selectivity from the decomposition of all three hydroxybenzaldehydes. The phenol selectivity was typically 100 ± 20% with the outliers being largely confined to experiments with low (<15%) conversions.

Table 4: *o*-hydroxybenzaldehyde thermolysis in SCW at 460°C and 250 atm.

	Concentration		Yield	
Residence Time (s)	*o*-HB (μmol/L)	Conversion (%)	Phenol (%)	Carbon Tally (%)
1.4	28.9	26.8	28.5	97.6
1.4	273.	12.4	4.4	91.3
1.4	344.	35.3	39.4	98.5
1.5	36.6	66.0	48.4	75.5
1.8	36.5	85.1	76.9	80.8
1.9	346.	42.3	46.9	97.9
2.3	272.	17.9	7.7	88.7
3.0	28.8	49.0	54.0	97.3
3.0	36.6	91.0	89.2	85.5
3.1	344.	61.0	66.1	95.5
6.6	37.2	100.	109.6	93.9
6.7	344.	91.	100.5	94.9
8.2	273.	34.6	16.2	79.2

Table 5: *m*-hydroxybenzaldehyde thermolysis in SCW at 460°C and 250 atm.

	Concentration		Yield	
Residence Time (s)	*m*-HB (μmol/L)	Conversion (%)	Phenol (%)	Carbon Tally (%)
1.1	92.2	5.1	2.3	96.9
1.9	92.2	10.5	2.9	92.0
3.0	421.	3.1	3.7	100.0
3.1	92.4	15.0	5.6	89.8
6.9	93.5	14.8	5.7	90.0
7.8	421.	9.0	8.7	98.5
10.2	59.7	7.6	8.0	99.3

Because the thermal decomposition of hydroxybenzaldehydes occurred on the same time scale as that anticipated for oxidation in supercritical water, we sought to quantify the thermal decomposition kinetics. That is we sought a power-law rate expression that could summarize the results of these pyrolysis experiments. We use power law kinetics, as shown in Equation 1, to be consistent with SCWO kinetics reported for other phenolic compounds (e.g., Gopalan and Savage, 1995; Martino et al., 1995; Kranjc and Levec, 1996; Martino and Savage, 1997).

$$rate = k[organic]^a \tag{1}$$

We write the concentration of the organic compound as a function of conversion, combine the rate law with the design equation for a plug-flow reactor, and integrate to obtain the expression in Equation 2 for the reactant conversion as a function of the process variables and the rate law parameters.

$$X = 1 - (1 + (a-1)k[organic]_o^{a-1}\tau)^{1/(1-a)} \qquad \text{for a} \neq 1 \tag{2}$$

We then use Equation 2 along with the nonlinear regression capabilities of SimuSolv (Steiner et al., 1990) to find the values of the parameters a and k that best represent the experimental data. SimuSolv performs the parameter estimation by the maximum likelihood method.

Table 6: *p*-hydroxybenzaldehyde thermolysis in SCW at 460°C and 250 atm.

	Concentration		Yield	
Residence Time (s)	*p*-HB (μmol/L)	Conversion (%)	Phenol (%)	Carbon Tally (%)
1.3	88.6	3.1	4.0	100.3
2.6	19.8	3.7	10.7	105.5
3.0	20.1	1.2	12.2	109.3
3.0	53.8	-1.5	4.4	105.3
3.0	464.	2.0	3.3	100.8
3.2	88.8	11.6	12.6	99.2
6.4	20.0	15.2	20.3	102.2
7.0	90.4	18.4	18.7	97.6
10.2	53.7	11.5	13.5	100.1
10.2	465.	8.3	10.2	100.4

We report the thermolysis rate laws for the hydroxybenzaldehydes below

$$r_{oHB} = 10^{-1.17\pm0.90}[oHB]^{0.86\pm0.22} \tag{3}$$

$$r_{mHB} = 10^{-3.57\pm0.68}[mHB]^{0.52\pm0.17} \tag{4}$$

$$r_{pHB} = 10^{-2.83\pm0.94}[pHB]^{0.80\pm0.22} \tag{5}$$

All rates in this report have units of moles/liter-second and the concentration is in moles/liter at the reaction conditions. All uncertainties in this report are the 95% confidence intervals.

We can compare the relative reactivity of the three hydroxybenzaldehydes by calculating pseudo-first-order rate constants from Equations 3 - 5 at a fixed hydroxybenzaldehyde concentration. For example, at 460°C, 250 atm, and a concentration of 250 μmol/L, the pseudo-first-order rate constants are 0.202 ± 0.069, 0.015 ± 0.003, and 0.0079 ± 0.0036 s^{-1}, for *o*-, *m*-, and *p*-hydroxybenzaldehyde, respectively. This comparison shows that the order of reactivity is *o*- > *m*- ≅ *p*-hydroxybenzaldehyde.

4.1.3 Thermolysis of Nitrophenols

Tables 7 – 9 contain the results of the SCW thermolysis of *o*-, *m*-, and *p*-nitrophenol. Each of the nitrophenols exhibited significant levels of conversion. Phenol was the only product consistently present in sufficiently high yields to quantify.

Table 7: *o*-nitrophenol thermolysis experiments in SCW at 460°C and 250 atm.

	Concentration		Yield	
Residence Time (s)	*o*-NP (μmol/L)	Conversion (%)	Phenol (%)	Carbon Tally (%)
1.3	93.4	36.7	6.6	70.0
1.3	437.	44.4	6.0	61.6
3.1	93.4	87.4	9.3	21.9
4.1	440.	93.0	15.3	22.3
6.0	93.4	100.0	8.7	8.7

Table 8: *m*-nitrophenol thermolysis experiments in SCW at 460°C and 250 atm.

	Concentration		Yield	
Residence Time (s)	*m*-NP (μmol/L)	Conversion (%)	Phenol (%)	Carbon Tally (%)
1.3	69.1	4.6	tr.	95.4
1.3	739.	0.9	tr.	99.1
3.0	69.0	10.1	6.5	96.4
3.1	739.	5.3	0.9	95.6
5.9	69.3	36.5	7.6	71.0
5.5	738.	15.5	5.5	90.0

Table 7 shows that *o*-nitrophenol attained complete conversion at a residence time of only six seconds. Since phenol was formed in yields of only around 10%, we sought the identities of additional liquid-phase products through GC-MS analysis using the protocol described by Martino

et al. (1995). This effort allowed us to identify products such as *p*-nitrophenol, benzoxazole, 2-methylbenzoxazole, indanone, dibenzofuran, and 2-phenoxyphenol in trace levels. Since the concentrations of these compounds was very low, however, they are not likely to account for a significant portion of the carbon atoms reacted. Moreover, the *o*-nitrophenol reactions did not produce a measurable gas flow. This absence of detectable reaction products in the reactor effluent, coupled with nearly complete conversion of *o*-nitrophenol, caused the carbon tally to fall far short of 100%.

Table 9: *p*-nitrophenol thermolysis experiments in SCW at 460°C and 250 atm.

	Concentration		Yield	
Residence Time (s)	*p*-NP (μmol/L)	Conversion (%)	Phenol (%)	Carbon Tally (%)
1.1	198.	22.9	6.9	83.9
1.3	73.0	14.7	5.7	91.0
1.4	704.	17.8	4.8	87.0
2.0	198.	32.0	12.3	80.3
3.0	73.1	24.1	9.7	85.6
3.0	692.	27.9	6.4	78.5
6.5	73.1	39.9	17.7	77.7
6.2	702.	62.4	11.4	49.0

p-Nitrophenol also had high conversions in SCW without the addition of oxygen (see Table 9). The phenol yields from these *p*-nitrophenol reactions were roughly the same as those observed from the thermolysis of *o*-nitropehnol, in spite of the *p*-nitrophenol conversions being lower. Through GC-MS analysis, we were able to identify *o*-nitrophenol and dibenzofuran as products in the aqueous effluent from the reactor. As was the case for the *o*-nitrophenol reactions, most of the reacted carbon in *p*-nitrophenol did not appear in aqueous-phase or gas-phase products, which caused consistently low values for the carbon tally. Some of this reacted carbon appeared to form solid products that remained in the reactor system, for we detected a gray/black powder on the filter located downstream of the reactor between the heat exchanger and the back-pressure regulator. We recovered some of this material and dissolved a portion of it in dichloromethane and analyzed it through GC-MS. It contained several compounds of greater molecular weight than the nitrophenol reactant. These compounds include dibenzofuran, 2-nitrodibenzofuran, and 4-phenoxyphenol. The formation of these high-molecular-weight products and their subsequent deposition in the reactor system might account for the balance of the reacted carbon in these nitrophenol experiments.

m-Nitrophenol displayed the lowest reactivity of the nitrophenols in SCW. With three of the six experiments having conversions that exceed 10%, however, the rate of pyrolysis appears to be

great enough to be significant at SCW oxidation conditions. Phenol formed from the thermolysis of *m*-nitrophenol, but not to a sufficient extent to account for all of the reacted carbon. *p*-Nitrophenol was the only additional liquid-phase product identified with GC-MS. As with the *p*-nitrophenol reactions, *m*-nitrophenol thermolysis formed a gel-like solid residue on the product filter. This residue contained dibenzofuran and 3-nitrodibenzofuran along with other unidentified compounds.

Because the nitrophenols are reactive under the conditions investigated, we used the experimental data to develop global reaction rate laws for the thermal decomposition of nitrophenols in SCW. The global rate expressions that best describe the experimental data in Tables 7 - 9 are

$$r_{oNP} = 10^{-0.61\pm0.54}[oNP]^{0.92\pm0.13} \tag{6}$$

$$r_{mNP} = 10^{-2.82\pm0.61}[mNP]^{0.63\pm0.16} \tag{7}$$

$$r_{pNP} = 10^{-0.40\pm0.23}[pNP]^{1.15\pm0.06} \tag{8}$$

We can compare the relative reactivity of the three nitrophenols by calculating pseudo-first-order rate constants from Equations 6 - 8 at a fixed nitrophenol concentration. For example, at a nitrophenol concentration of 250 μmol/L, the pseudo-first-order rate constants are 0.460 ± 0.071, 0.032 ± 0.007, and 0.117 ± 0.009 s^{-1}, for *o*-, *m*-, and *p*-nitrophenol, respectively. This comparison shows that the order of reactivity is *o*- > *p*- > *m*-nitrophenol. This ranking is consistent with that observed for the hydroxybenzaldehydes in that the *o*-substituted phenol is the most reactive in both cases. The pseudo-first-order rate constants for the nitrophenols exceed those for the corresponding hydroxybenzaldehyde, which reveals that NO_2-substituted phenols are more reactive in SCW than CHO-substituted phenols.

4.1.4 Thermolysis of Benzenediols

Table 10 displays the results from the thermolysis of resorcinol, 1,3-dihydroxybenzene, in SCW. With residence times ranging from 1.3 to 7.2 seconds, the greatest reactant conversion observed was 10.1%. This level of pyrolysis is not likely to be significant when compared to the oxidation rate expected at this temperature. Thus, no further experiments or data analysis was deemed necessary. We were unable to identify any products from the reactions of resorcinol in SCW under these conditions.

We also attempted thermolysis experiments with catechol (1,2-dihydroxybenzene) and hydroquinone (1,4-dihydroxybenzene), but these compounds appeared to be unstable in aqueous solutions even at ambient conditions. Stock solutions of these compounds significantly decomposed in the approximately 24 hours of time it took to complete the reaction and perform the effluent analysis. This behavior made it difficult to obtain reliable results from experiments with these compounds.

Table 10: Resorcinol thermolysis experiments in SCW at 460°C and 250 atm.

	Concentration	
Residence Time (s)	resorcinol (μmol/L)	Conversion (%)
1.4	105.4	1.2
1.3	1001.	10.1
3.2	106.3	6.8
3.2	1001.	10.1
6.9	1000.	5.9
7.2	105.4	6.8

4.2 SCWO GLOBAL KINETICS

The previous section provided results from thermolysis (no oxygen) studies. This section provides the results of SCWO experiments with cresols and hydroxybenzaldehydes, and an analysis of those results, which led to global reaction rate laws for each compound. Our approach is to model the global kinetics using a power-law rate expression of the form

$$rate = A\, e^{\frac{-E_a}{RT}} [organic]^a [O_2]^b [H_2O]^c. \qquad (9)$$

We restrict our kinetics experiments to those wherein the oxygen concentration remains essentially constant throughout the reaction (O_2 present in at least 200% stoichiometric excess), in which case the differential equation that describes the reactant conversion in an isothermal, isobaric, plug-flow reactor can be solved analytically for the conversion to yield

$$X = 1 - \left(1 + (a-1) A e^{-E_a/RT} [organic]_o^{a-1} [O_2]_o^b [H_2O]_o^c \tau\right)^{1/1-a} \quad \text{for a} \neq 1 \quad (10)$$

We then fit the experimental data to this non-linear algebraic equation to estimate numerical values for the rate-law parameters.

4.2.1 Cresol Oxidation Kinetics

In this section we revise our previously reported rate equation for o-cresol SCWO (Martino et al., 1995) because we discovered that the *o*-cresol conversion was not measured accurately by our previous HPLC analysis. One of the major products from *o*-cresol SCWO, *o*-hydroxybenzaldehyde, eluted from the HPLC column at the same time as the reactant. This previously undiscovered overlap of reactant and product peaks led to conversions that were systematically low. We are able to correct this problem and calculate accurate values for the *o*-cresol conversions because the molar yields of *o*-hydroxybenzaldehyde had been previously measured by a complementary GC analysis. These data, along with the HPLC response factors for *o*-cresol and *o*-hydroxybenzaldehyde, were used to calculate corrected values for the *o*-cresol conversion. Table 11 shows the revised values for the *o*-cresol conversion and the carbon tally, which we calculate as the percentage of carbon atoms flowing into the reactor that appear in the reaction products we quantify.

The parameters in the global rate law for *o*-cresol disappearance were reevaluated using these revised data and the SimuSolv software package. The resulting global rate equation is

$$r_{oCR} = 10^{7.1\pm2.4}\exp\left(\frac{-33700\pm9600}{RT}\right)[oCR]^{0.54\pm0.14}[O_2]^{0.35\pm0.22}[H_2O]^{1.46\pm0.69} \qquad (11)$$

We also investigated the oxidation of the *m*- and *p*-methylphenols in supercritical water at a single temperature and pressure of T = 460 °C and P = 250 atm. Tables 12 and 13 provide the experimental conditions and the results.

The data for *m*- and *p*-cresol were fit to a global rate expression of the form

$$rate = k[organic]^a[O_2]^b \qquad (12)$$

The resulting parameters and their 95% confidence intervals are

$$r_{mCR} = 10^{-1.43\pm0.48}[mCR]^{0.65\pm0.09}[O_2]^{0.61\pm0.24} \qquad (13)$$

$$r_{pCR} = 10^{-1.55\pm0.40}[pCR]^{0.60\pm0.07}[O_2]^{0.54\pm0.17} \qquad (14)$$

Table 11: Revised data for SCWO of *o*-cresol

Temperature (°C)	Pressure (atm)	Residence Time (s)	Concentration *o*-cresol (μmol/L)	Concentration O_2 (mmol/L)	Reported Conversion (%)	Corrections Conversion (%)	Corrections Carbon Tally (%)
350.0	250	29.5	588.	42.6	98.4	98.6	52.5
370.0	250	25.1	543.	36.6	98.0	98.4	49.5
380.2	250	15.6	413.	31.4	72.7	74.9	61.5
380.9	250	20.7	412.	29.0	78.1	80.3	55.4
379.6	250	46.3	416.	32.4	99.5	99.6	64.5
400.2	250	8.0	173.	11.6	30.4	33.8	86.1
420.4	250	4.6	123.	9.25	18.7	26.1	110.2
420.6	251	6.3	128.	9.13	29.6	34.6	98.0
420.5	250	13.2	120.	9.28	51.7	54.5	86.9
440.3	250	5.5	117.	7.82	44.0	51.2	95.0
460.1	200	3.6	81.7	5.20	40.5	49.6	112.6
460.2	220	4.1	79.1	5.92	42.5	55.2	124.3
460.2	230	4.4	99.1	6.31	44.3	53.0	112.2
460.3	240	4.7	89.6.	6.73	41.0	48.3	108.5
459.0	250	0.5	180.	5.19	10.8	12.9	102.9
460.0	250	0.6	44.7.	4.03	20.3	24.1	99.2
460.4	250	0.9	327.	9.07	6.4	9.6	n.d.
460.0	250	0.9	46.6	3.90	23.9	30.5	108.4
459.9	250	0.9	159.	5.85	7.2	11.3	110.4
460.0	250	1.2	106.	7.52	29.4	34.0	103.5
460.0	250	1.2	30.7	5.08	47.0	52.3	116.1
460.0	250	2.0	30.9	9.23	66.3	74.0	105.2
460.0	250	2.1	313.	9.31	32.7	36.5	89.3
460.3	251	3.7	117.	6.64	56.3	64.3	95.8
460.2	250	4.3	253.	10.8	34.2	38.0	99.2
460.3	250	4.4	23.5	1.19	61.0	67.0	91.7
460.2	250	4.4	184.	4.87	47.3	57.6	101.4
460.7	250	5.3	269.	10.1	34.5	44.3	115.8
461.1	250	5.3	116.	7.10	76.0	83.8	102.6
459.9	250	5.4	23.1	1.21	63.6	68.6	86.4
459.9	250	5.4	437.	7.80	40.9	44.6	90.9
460.1	250	5.5	364.	9.22	41.9	50.9	103.0
460.1	250	5.5	44.2	2.46	67.9	72.3	94.2
460.0	251	5.9	156.	5.44	67.4	73.5	96.4
462.3	251	7.3	260.	10.3	52.6	61.7	100.5
459.9	251	7.7	170.	5.09	76.7	85.0	101.9
460.0	250	7.7	419.	8.09	55.1	60.0	88.0
460.4	252	7.7	44.3.	2.49	83.4	85.5	76.0
459.5	250	7.9	103.	7.44	83.4	87.0	102.0
460.5	250	9.0	314.	9.30	58.5	65.3	98.4
460.9	250	11.0	102.	7.37	96.4	97.9	96.0
460.0	250	12.0	459.	7.44	72.1	75.0	77.3
459.9	250	12.2	172.	4.91	94.7	96.8	87.1
460.0	251	12.6	45.3	2.41	97.6	98.4	82.5
459.8	251	12.9	22.0	1.27	88.1	90.1	99.7
460.0	260	5.3	101.	7.59	52.3	59.0	105.5
459.8	270	5.7	126.	8.05	64.5	67.3	123.9
460.1	280	6.0	113.	8.51	62.5	69.8	106.8
459.5	300	6.9	151.	9.61	77.0	82.2	101.5
480.9	250	4.5	92.6	6.55	85.0	87.7	93.4
499.7	250	4.3	86.8	6.15	98.3	98.6	97.3

Table 12: Results from SCWO of *m*-cresol at 460°C and 250 atm

	Initial Concentration			Product Molar Yields				
Res. Time (s)	*m*-cresol (μmol/L)	O_2 (mmol/L)	Conv. (%)	CO_2 (%)	CO (%)	*m*-HB (%)	Phenol (%)	Carbon Tally (%)
3.5	356.	9.03	11.3	2.0	0.8	0.9	0.0	92.4
5.0	38.4	5.03	20.3	7.1	1.2	0.0	0.0	88.0
5.0	46.0	9.38	29.4	10.4	2.5	1.3	0.0	84.7
5.0	180.	9.35	23.7	4.2	3.4	1.2	0.0	85.2
5.1	106.	5.16	10.7	2.6	1.3	1.4	0.0	94.6
5.1	343.	8.95	12.6	n.d.	n.d.	1.5	0.2	n.d.
7.4	59.5	3.80	23.8	10.7	0.6	1.8	0.0	89.3
7.4	270.	7.04	24.1	4.4	1.4	1.5	0.3	83.5
7.5	69.6	7.14	34.3	9.5	3.0	1.0	0.0	79.2
7.5	172.	3.83	20.8	3.0	0.7	1.6	0.0	84.6
7.5	303.	9.73	18.1	7.4	2.2	2.1	0.4	93.9
7.5	498.	6.89	14.0	3.6	1.2	1.9	0.4	93.0
10.2	311.	9.29	34.9	9.6	2.9	3.3	0.8	81.7

Table 13: Results from SCWO of *p*-cresol at 460°C and 250 atm.

	Initial Concentration			Product Yields				
Res. Time (s)	*p*-cresol (μmol/L)	O_2 (mmol/L)	Conv. (%)	CO_2 (%)	CO (%)	*p*-HB (%)	Phenol (%)	Carbon Tally (%)
3.5	351.	9.42	21.7	n.d.	n.d.	4.9	0.2	n.d.
4.9	33.4	9.27	51.0	10.2	4.8	21.6	2.6	87.7
4.9	42.6	5.07	40.4	11.9	2.3	14.9	1.7	90.2
4.9	103.	9.19	42.3	4.4	3.3	12.5	1.1	78.8
4.9	107.	5.07	29.5	n.d.	n.d.	6.2	0.0	n.d.
5.5	359.	8.72	18.0	2.8	1.6	6.4	0.5	93.2
7.3	52.2	7.02	58.2	13.6	4.4	20.6	3.4	83.3
7.3	314.	9.94	41.9	n.d.	1.4	12.3	1.2	n.d.
7.4	63.0	3.91	38.2	5.3	2.3	13.8	1.6	84.5
7.4	154.	7.10	42.8	n.d.	n.d.	11.9	1.2	n.d.
7.4	157.	3.92	32.4	4.1	1.3	7.7	0.7	81.3
10.5	293.	9.43	43.9	7.1	2.8	14.6	1.9	82.2

4.2.2 Hydroxybenzaldehyde Oxidation Kinetics

The data from the SCWO experiments for *o*-, *m*-, and *p*-hydroxybenzaldehydes, which appear in Tables 14 - 16, were treated in the same manner as the data from the *m*- and *p*-cresol experiments.

Table 14: Results from SCWO of *o*-hydroxybenzaldehyde at 460°C and 250 atm.

	Initial Concentration			Product Yields			
Res. Time (s)	*o*-HB (μmol/L)	O_2 (mmol/L)	Conv. (%)	CO_2 (%)	CO (%)	Phenol (%)	Carbon Tally (%)
0.54	30.4	6.34	84.0	35.1	1.6	59.8	103.9
0.55	272.	6.44	52.6	11.8	0.9	31.6	87.1
0.68	25.2	4.18	84.0	19.6	2.2	51.3	81.7
0.68	290.	4.17	41.5	4.5	1.0	19.3	80.5
0.71	71.0	3.83	84.9	24.2	0.8	43.7	77.5
1.4	27.3	6.99	100.0	43.3	4.2	90.9	125.4
1.4	65.5	3.67	100.0	19.5	1.1	65.7	76.9
1.4	261.	6.74	65.8	10.9	1.9	42.4	83.3
1.5	25.7	4.15	100.0	23.5	3.3	69.4	86.2
1.5	293.	4.17	46.8	4.6	2.2	15.4	73..2
1.6	91.0	3.89	56.3	21.8	3.2	56.5	117.1

Table 15: Results from SCWO of *m*-hydroxybenzaldehyde at 460°C and 250 atm.

	Initial Concentration			Product Yields			
Res. Time (s)	*m*-HB (μmol/L)	O_2 (mmol/L)	Conv. (%)	CO2 (%)	CO (%)	Phenol (%)	Carbon Tally (%)
0.54	95.3	4.66	22.3	10.6	0.7	0.7	89.6
0.67	75.1	6.86	1.0	5.0	0.2	0.0	104.3
0.67	305.	6.92	1.0	1.2	0.3	0.8	101.2
0.68	23.5	6.97	4.9	0.0	0.0	0.0	95.1
0.71	81.5	3.32	19.1	3.8	0.5	0.0	85.3
0.91	88.6	5.06	31.8	18.9	1.2	1.2	89.3
1.4	74.7	3.68	18.7	n.d.	n.d.	2.1	n.d.
1.4	301.	7.08	8.3	4.1	1.2	2.3	99.0
1.5	23.1	7.14	23.8	17.9	0.6	0.0	94.7
1.5	23.7.	2.96	14.7	n.d.	n.d.	0.0	n.d.
1.5	71.9.	7.23	8.4	8.1	1.2	2.0	102.6
1.5	84.5	5.36	27.1	14.0	2.0	2.3	90.8
1.5	255.	2.94	19.5	10.4	2.1	4.1	96.5
3.1	90.6	5.00	54.3	24.9	3.8	2.4	76.5
4.1	14.8	3.68	29.4	23.8	0.0	5.2	98.9
4.1	66.1	2.49	20.1	7.7	0.8	2.6	90.5
4.1	162.	3.66	18.2	5.9	0.9	2.8	91.1
10.2	32.9	6.02	48.4	27.6	3.6	6.0	87.9
10.2	79.7	8.92	62.6	34.6	3.6	6.7	81.3
10.3	71.9	8.98	80.9	97.8	0.0	0.0	117.0

Table 16: Results from SCWO of *p*-hydroxybenzaldehyde at 460°C and 250 atm.

	Initial Concentration			Product Yields			
Res. Time (s)	*p*-HB (μmol/L)	O_2 (mmol/L)	Conversion (%)	CO_2 (%)	CO (%)	Phenol (%)	Carbon Tally (%)
0.72	74.8	5.64	16.5	6.8	0.0	6.1	95.5
0.92	19.3	2.96	40.2	16.0	0.0	17.3	90.7
0.92	21.0	7.21	18.2	19.4	0.0	7.4	107.6
0.92	203.	7.18	11.8	4.3	0.0	6.4	98.1
0.93	68.4	5.43	14.1	6.9	0.0	6.6	98.5
0.94	63.4	3.02	15.4	4.4	0.0	5.4	93.7
1.5	67.5	5.56	23.8	7.2	0.0	12.7	94.3
3.1	17.2	3.34	64.2	29.6	0.0	28.4	89.8
3.1	19.6	7.72	41.1	30.9	0.0	21.7	108.4
3.1	186.	7.74	32.7	13.6	0.0	15.4	94.0
3.1	57.1	3.41	38.5	15.3	0.0	18.2	92.4
3.2	68.7	5.44	46.4	16.5	0.0	17.1	84.7
4.0	71.5	2.34	24.5	6.3	0.4	19.2	98.2
10.2	35.1	6.00	76.2	28.8	1.5	62.0	105.7

The global rate expressions for the hydroxybenzaldehydes at T = 460 °C and P = 250 atm. are

$$r_{oHB} = 10^{-0.78\pm1.10}[oHB]^{0.47\pm0.09}[O_2]^{0.57\pm0.47} \quad (15)$$

$$r_{mHB} = 10^{-2.57\pm1.12}[mHB]^{0.75\pm0.15}[O_2]^{-0.13\pm0.22} \quad (16)$$

$$r_{pHB} = 10^{-1.81\pm0.57}[pHB]^{0.77\pm0.10}[O_2]^{-0.02\pm0.19} \quad (17)$$

The rate expressions of Equation 15 - 17 describe the net rate of disappearance of the particular hydroxybenzaldehyde through all competing reactions. At SCWO conditions, these competing reactions can include pyrolytic and hydrolytic decomposition in addition to oxidative destruction. We desired to separate the contributions from pyrolysis and oxidation so that we could determine the kinetics of the oxidation reaction alone. To accomplish this separation, we write the total rate of disappearance of hydroxybenzaldehyde as the sum of the rate of pyrolysis plus the rate of oxidation.

$$rate = rate_{pyrolysis} + rate_{oxidation} = k_p[organic]^{a_p} + k_o[organic]^{a_o}[O_2]^{b_o} \quad (18)$$

The previous section provided rate laws for the pyrolytic contribution, so the parameters k_P and a_P are known. Thus, we used these parameters and the experimental data in Tables 14-16 to estimate values of k_O, a_O, and b_O in Equation 18.

We integrated the governing differential equation numerically, and simultaneously performed the parameter estimation. The objective function was the sum of the squares of the differences between calculated and experimental hydroxybenzaldehyde conversions. The results of this analysis appear below.

$$r_{oHB} = 10^{-1.17}[oHB]^{0.86} + 10^{-0.98}[oHB]^{0.39}[O_2]^{0.68} \quad (19)$$

$$r_{mHB} = 10^{-3.57}[mHB]^{0.52} + 10^{-0.99}[mHB]^{1.37}[O_2]^{0.28} \quad (20)$$

$$r_{pHB} = 10^{-2.83}[pHB]^{0.80} + 10^{-2.01}[pHB]^{0.72}[O_2]^{0.02} \quad (21)$$

4.3 STRUCTURE AND REACTIVITY

In this section we use the rate laws reported here for cresols and hydroxybenzaldehydes, along with those in the literature for phenol and *o*-chlorophenol to calculate pseudo-first-order rate constants for SCWO of each phenolic compound under identical conditions. For the hydroxybenzaldehydes, which disappear through both thermal and oxidation reactions, we calculated the pseudo-first-order rate constant from the second term in Equations 19 - 21 so that it excludes the thermal component. All of these pseudo-first-order rate constants, k'', were calculated at reactant concentrations of *[organic]* = 10^{-4} M and *[O2]* = 7×10^{-3} M, which fell within the range of conditions studied experimentally. Table 17 provides these rate constants.

Table 17: Pseudo-First-Order Rate Constants for SCWO of Phenolic Compounds at 460°C and 250 atm, with [Organic] = 100 μmol/liter and [O_2] = 7 mmol/liter.

Compound	k'' *(1/s)*
phenol (Gopalan and Savage, 1995b)	0.0308
o-chlorophenol (Li et al., 1993)	0.0379
o-cresol	0.179 ± 0.023
m-cresol	0.0423 ± 0.0028
p-cresol	0.0754 ± 0.0041
o-hydroxybenzaldehyde[2] (Eqn. 19)	0.939
m-hydroxybenzaldehyde[2] (Eqn. 20)	0.0842
p-hydroxybenzaldehyde[2] (Eqn. 21)	0.117

By comparing the values of k'' in Table 17, we can in effect compare the reaction rates for these phenolic compounds at this particular set of conditions. Table 17 reveals that all of the substituted phenols that have been studied thus far in our laboratory oxidize more quickly than phenol itself, with *o*-chlorophenol being the most resistant of the substituted phenols studied. This observation suggests that phenol is a good "worst-case" compound to use in evaluations of SCWO, because

most other phenolic compounds will be easier to treat. Table 17 also reveals that the location of the substituent influences the reactivity of the substituted phenol in supercritical water. For both the cresols and the hydroxybenzaldehydes, the *ortho* isomer has the highest rate of reaction and the *meta* isomer has the lowest. Finally, the data in Table 17 show that the identity of the substituent influences the reaction rates. For example, the relative reactivity of *o*-substituted phenols is 1, 1.2, 5.8, 39 as the group resident at the *ortho* position varies through the sequence -H, -Cl, $-CH_3$, and -CHO, respectively.

4.4 OXIDATION PRODUCTS AND PATHWAYS

Tables 12 - 13 and 14 - 16 provide quantitative data for the molar yields of reaction products from SCWO of cresols and hydroxybenzaldehydes. The yields of CO, CO_2, and hydroxybenzaldehydes are normalized molar yields in the sense that if there were complete conversion of the reactant to only one particular carbon-containing product, the molar yield of that product would be 100%. The molar yields of CO and CO_2 from cresol SCWO, for example, were calculated as the molar flow rate of CO or CO_2 in the reactor effluent divided by seven times the molar flow rate of cresol (since each cresol molecule has seven carbon atoms) in the reactor feed. The molar yield of phenol was not normalized in this manner, but rather was calculated as the molar flow rate of phenol in the reactor effluent divided by the molar flow rate of reactant in the reactor feed stream.

4.4.1 SCWO of Cresols

Our previous work with *o*-cresol oxidation identified 19 intermediate liquid-phase products and detected the presence of ten additional compounds (Martino et al., 1995). Our present results from *m*- and *p*-cresol SCWO do not display such a rich product spectrum. We detected relatively few products of incomplete oxidation from *m*- and *p*-cresol. Other than phenol and the corresponding hydroxybenzaldehydes, for which Tables 12 and 13 provide quantitative data, the only product we detected was indanone.

Tables 12 and 13, along with our previous results for o-cresol (Martino et al., 1995), provide considerable insight into the governing reaction network for SCWO of cresols and the relative rates of the different paths. These data show that for all three cresols, the yield of CO_2 always exceeded the yield of CO. This behavior has also been observed for the SCWO of phenol and *o*-chlorophenol (Li et al., 1992). The yield of CO_2 consistently exceeding the yield of CO for all phenolic compounds studied to date indicates that CO is not an important intermediate in the reaction network for CO_2 production from phenolic compounds. Rather, there must be some path

for CO_2 formation that bypasses CO. A strong possibility is decarboxylation of carboxylic acid intermediates formed via ring-opening reactions.

A second trend that all three cresols display is that at cresol conversions of less than 50% the yield of the hydroxybenzaldehyde always exceeds the yield of phenol. This behavior demonstrates that oxidation of the $-CH_3$ substituent in cresols is favored over elimination of the substituent.

Comparing the yields of CO and CO_2 with the yield of phenol reveals that *o*-cresol is unique in that these yields are comparable, even at the lower *o*-cresol conversions. For both *m*- and *p*-cresol, on the other hand, the yield of CO + CO_2 is much greater than the yield of phenol. This observation indicates that elimination of the *ortho* substituent (from *o*-cresol or perhaps the *o*-hydroxybenzaldehyde product) is more facile than elimination of the analogous *m*- and *p*-substituent. The *m*- and *p*-cresols appear to favor ring-opening reactions and CO_x formation over elimination of the substituent. This difference in the relative reactivity for these competing pathways is consistent with the dissociation energy of the C-C bond in *o*-substituted phenols being lower than that in *m*- and *p*-substituted phenols.

A final observation we can make is that hydroxybenzaldehydes are the major low-conversion products from SCWO of *o*- and *p*-cresol whereas CO and CO_2 are the most abundant products from *m*-cresol SCWO. This difference indicates that the $-CH_3$ substituent in *o*- and *p*-cresol is more readily attacked and oxidized than is the $-CH_3$ substituent in *m*-cresol. This difference can be understood by recognizing that a carbon-centered radical at the *o*- or *p*- position enjoys a greater resonance stabilization than does an analogous radical at the *m*-position.

To summarize this section, we offer Figure 1 as a general reaction network for SCWO of cresols. This network shows three parallel paths for cresol SCWO. One leads to a hydroxybenzaldehyde via oxidation of the methyl substituent, another leads to ring-opening products and the formation of CO and CO_2, and the last leads to phenol via demethylation. The relative importance of the parallel pathways depends on the specific cresol isomer being oxidized.

Figure 1 shows that phenol and hydroxybenzaldehydes are key organic intermediates in the reaction network, so the network can be expanded by including the reaction paths for these compounds. The SCWO of phenol has been thoroughly investigated and a proven reaction network is available in the literature (Gopalan and Savage, 1995b). This network proceeds through two parallel primary paths that produce either phenol dimers or ring-opening products. Both the dimers and the ring-opening products are ultimately oxidized to CO_2. The SCWO of

hydroxybenzaldehydes, on the other hand, has been unexplored until now. The next section, which discusses the reaction network for SCWO of hydroxybenzaldehydes, will thus allow us to complete the reaction network for SCWO of cresols.

4.4.2 SCWO of Hydroxybenzaldehydes

Tables 14-16 show that the major products from SCWO of hydroxybenzaldehydes were CO, CO_2, and phenol. The data in these Tables reveal that for all three hydroxybenzaldehydes, the molar yield of CO_2 always exceeded that of CO. This observation is fully consistent with the SCWO behavior of all other phenols studied to date. The data also show that although all three hydroxybenzaldehydes led to the same products, the relative abundance of the different products varied for the three isomers. For *o*-hydroxybenzaldehyde the yield of phenol was greater than the yield of CO_x, for *m*-hydroxybenzaldehyde the yield of CO_x was greater than the yield of phenol, and for *p*-hydroxybenzaldehyde the yields of CO_x and phenol were comparable. Phenol formation from hydroxybenzaldehydes involves loss of the CHO group, and a higher phenol yield from *o*-hydroxybenzaldehyde is consistent with the *o*-C-C bond being weaker than the *m*- and *p*-C-C bonds.

Figure 2 summarizes this discussion of hydroxybenzaldehyde products and pathways by showing a reaction network for hydroxybenzaldehyde SCWO. There are two parallel reactions. One leads to phenol and the other leads to ring-opening reactions and ultimately CO_2. We can combine the reaction network in Figure 2 for hydroxybenzaldehydes, the reaction network for phenol in the literature (Gopalan and Savage, 1995b), and the reaction network in Figure 1 for cresols to assemble a more complete reaction network that shows the conversion of cresols and its important intermediate byproducts into CO_2. Figure 3 provides this overall reaction network for the SCWO of cresols.

5. SUMMARY AND CONCLUSIONS

Cresols are largely stable in SCW at 460°C and 250 atm for residence times up to about 30 seconds. In contrast, hydroxybenzaldehydes and nitrophenols are reactive under these conditions. Thus, treatment of these compounds by SCW oxidation will involve a significant purely thermal component, which implies that much of the oxidation will be of the thermal reaction products (such as phenol) rather than the substituted phenol itself.

For phenols with CHO and NO_2 substituents, the *o*-substituted isomer is the most reactive in SCW. For a given substituent location, nitrophenols are more reactive than hydroxy-

benzaldehydes, which are much more reactive than cresols. Thus, there are clearly substituent effects on the reactivity of substituted phenols in SCW. This observation suggests that quantitative structure-reactivity relations might be available for this class of compounds.

The oxidation of CH_3- and CHO-substituted phenols in supercritical water proceeds more rapidly than the oxidation of phenol itself. For a given substituent, *o*-substituted phenols are the most reactive, and *m*-substituted phenols are least reactive. For a given point of substitution, CHO-substituted phenols are more reactive than CH_3-substituted phenols. Quantitative reaction rate laws for each phenolic compound appear in this paper.

The oxidation of cresols in supercritical water proceeds through three parallel paths, demethylation (to form phenol), oxidation of the methyl group (to form hydroxybenzaldehyde), and ring-opening. The ring-opening path most likely proceeds through carboxylic acid intermediates, the decarboxylation of which account for the high yields of CO_2. The relative rates of the three parallel paths are isomer specific and consistent with the bond energies and resonance stabilization expected in substituted phenols. The oxidation of hydroxybenzaldehydes in supercritical water proceeds through two parallel paths. One path leads to phenol and the other involves ring-opening and CO_2 formation.

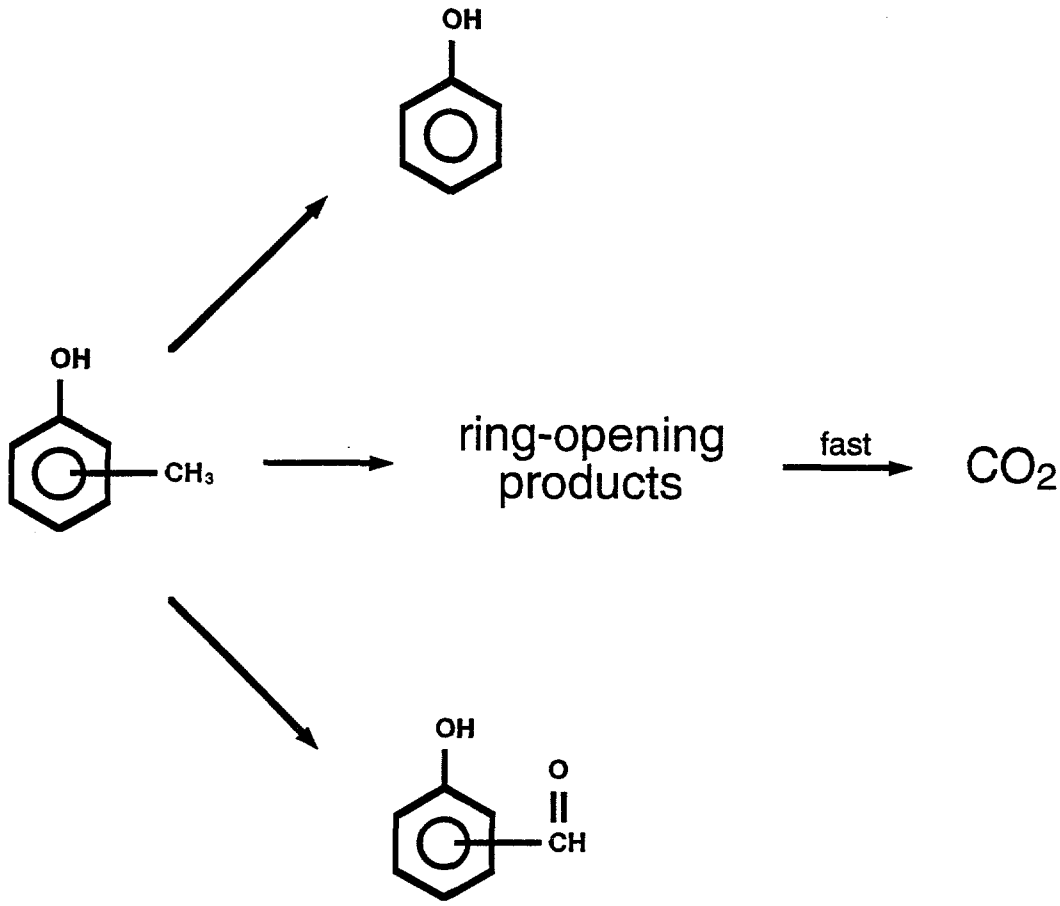

Figure 1: Cresol SCWO Pathways

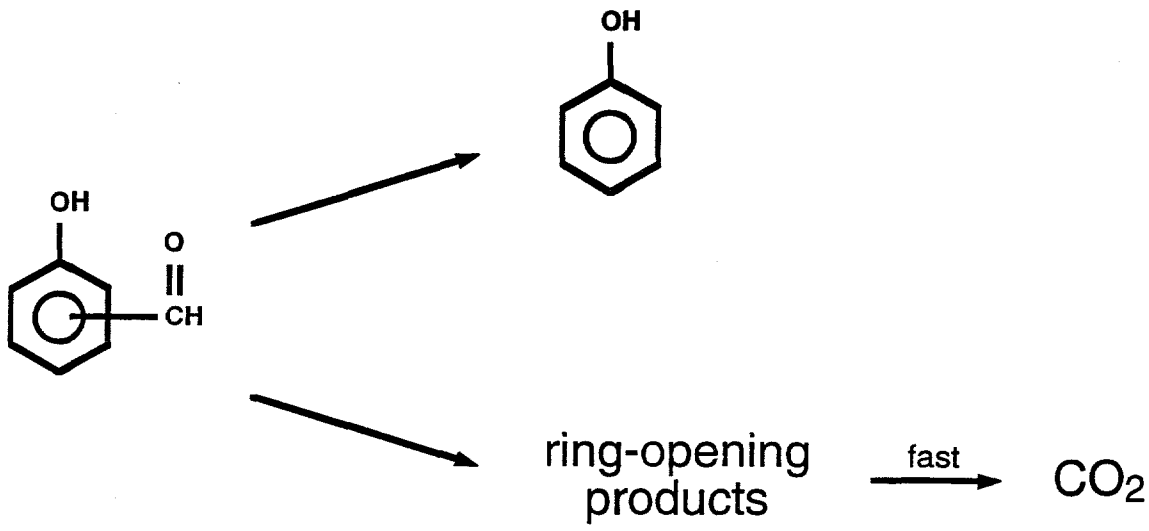

Figure 2: Hydroxybenzaldehyde SCWO Pathways

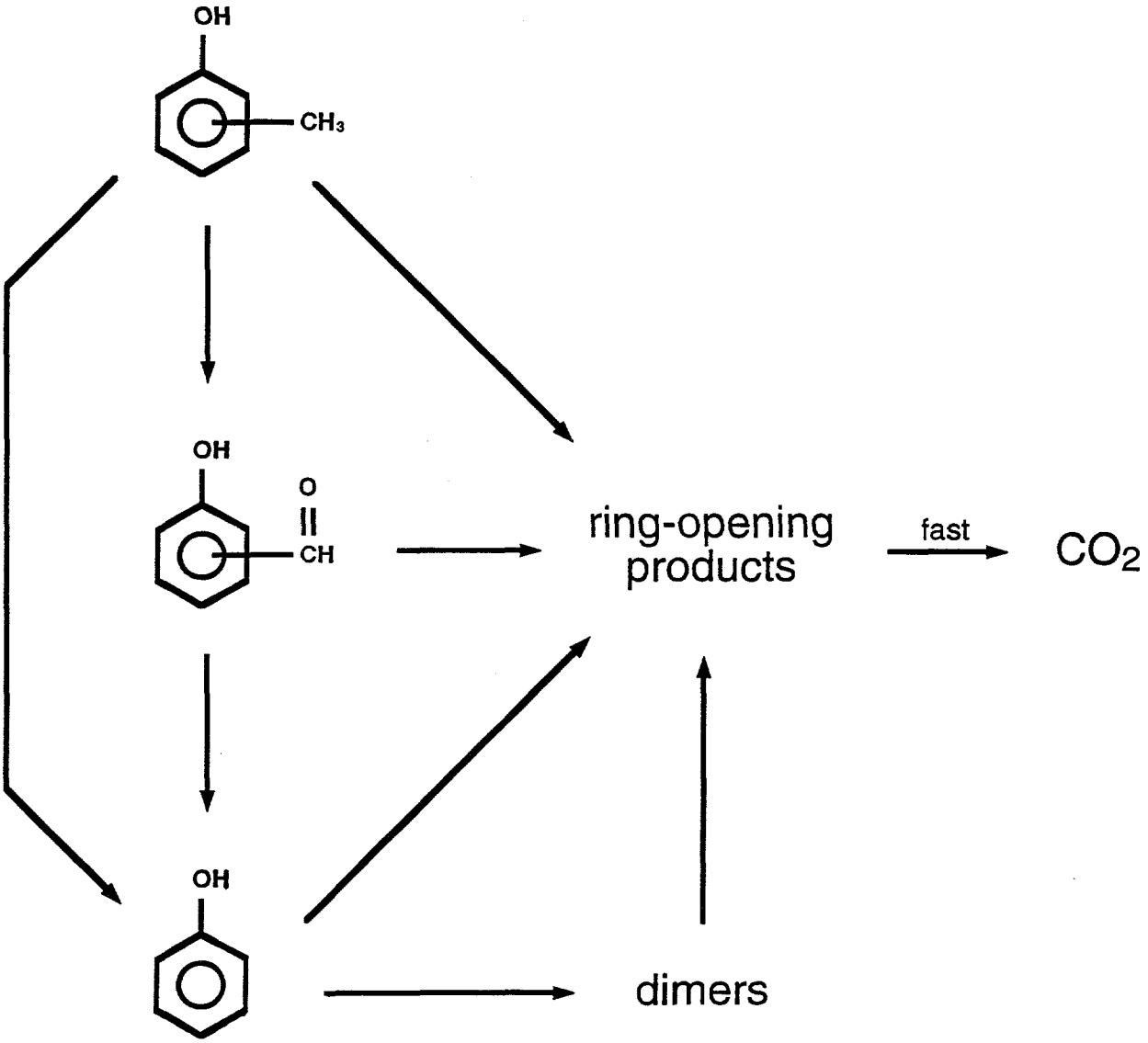

Figure 3: Complete SCWO Network for Cresols, Hydroxybenzaldehydes, and Phenol

6. NOMENCLATURE

A = Arrhenius preexponential factor

a = reaction order for the organic compound

b = reaction order for oxygen

c = reaction order for water

CI = confidence interval

CR = cresol (methylphenol)

E_a = activation energy

HB = hydroxybenzaldehyde

I.D. = inner diameter

k = reaction rate constant

k' = log(k)

k'' = pseudo-first-order rate constant

M = moles per liter

m = *meta-*

n = number of experiments

P = pressure

o = *ortho-*

O.D. = outer diameter

p = *para-*

P = pressure

r = rate

R = gas constant

T = absolute temperature

t = time

X = reactant conversion

Greek Letters

σ^2 = variance or covariance

τ = residence time

Subscripts

0 = at reactor entrance

o = oxidation

p = pyrolysis

c = critical value

7. REFERENCES

Gopalan, S.; Savage, P. E. in *Innovations in Supercritical Fluids*; Hutchenson, K. W.; Foster, N. R., Eds.; ACS Symposium Series 608; American Chemical Society: Washington, DC, 1995; pp 217-231, (1995a).

Gopalan, S.; Savage, P. E. Reaction Network for Phenol Oxidation in Supercritical Water: A Comprehensive Quantitative Model. *AIChE J.*, **1995**, *41*, 1864-1873.

Jevtitch, M. M.; Bhattacharyya, D. Biotreated Coal Liquefaction Wastewater: Identification of Organics by Composite RO Membrane Concentration, HPLC, and GC/MS. *Env. Prog.*, **1986**, *5*, 130-134.

Krajnc, M.; Levec, J. On the Kinetics of Phenol Oxidation in Supercritical Water. *AIChE J.*, **1996**, *42*, 1977-1984.

Martino, C. J.; Savage, P. E. Supercritical Water Oxidation Kinetics , Products, and Pathways for CH_3 and CHO Substituted Phenols. *Ind. Eng. Chem. Res.* **1997** (under review).

Martino, C. J.; Savage, P. E.; Kasiborski, J. Kinetics and Products from *o*-Cresol Oxidation in Supercritical Water. *Ind. Eng. Chem. Res.*, **1995**, *34*, 1941-1951.

Martino, C. J.; Savage, P. E. Thermal Decomposition of Substituted Phenols in Supercritical Water. *Ind. Eng. Chem. Res.* **1997**, (under review).

Modell, M. in *Standard Handbook of Hazardous Waste Treatment and Disposal*, Freeman, H. M., Ed.; McGraw Hill: New York, 1989, sec 8.11.

Savage, P. E.; Gopalan, S.; Mizan, T. I.; Martino, C. J.; Brock, E. E. Reactions at Supercritical Conditions: Fundamentals and Applications. *AIChE J.*, **1995**, *41*, 1723-1778.

Steiner, E. C.; Rey, T. D.; McCroskey, P. S. *SimuSolv Modeling and Simulation Software Reference Guide*; The Dow Chemical Company, Midland, MI 1990.

Yen, T. F.; Tang, J. I. S.; Washburne, M.; Cohanim, S. *Analytical Methods for Hazardous Organics in Liquid Wastes from Coal Gasification and Liquefaction Processes*, 1982; EPA-600/4-82-038.

Thornton, T. D.; Savage, P. E. Phenol Oxidation in Supercritical Water. *J. Supercritical Fluids*, **1990**, *3*, 240-248.